Trilepton Higgs signal at hadron colliders

Howard Baer[a][†] and James D. Wells[b][†]

(a) *Department of Physics, Florida State University*
Tallahassee, Fl 32306

(b) *Stanford Linear Accelerator Center, Stanford, Ca 94309*

Abstract

Determining the origin of electroweak symmetry breaking will be one of the primary functions of high energy colliders. We point out that most Higgs boson searches pursued at hadron colliders require Yukawa interactions either in the production or the decay of a Higgs boson. We propose a trilepton Higgs boson search based only upon the gauge interactions of the Higgs. This strategy can be utilized successfully for the standard model (SM) Higgs boson as well as non-standard Higgs bosons which break electroweak symmetry but have little to do with fermion mass generation. The trileptons come from Wh production followed by $Wh \to WWW^{(*)} \to 3l$ decays. A SM Higgs trilepton signal would be difficult to detect at the Tevatron collider: with 100 fb^{-1} of data, only a 3σ signal above background can be achieved after cuts if $140\,\text{GeV} < m_{h^0_{sm}} < 175\,\text{GeV}$. Some discrimination of signal over background can be gained by analyzing the opposite sign dilepton p_T distributions. At the LHC with 30 (100) fb^{-1} a clear discovery above the 5σ level is possible for a Higgs mass in the range $140 - 185$ $(125 - 200)\,\text{GeV}$. Prospects for a trilepton Higgs discovery are greatly improved for models with non-standard Higgs sectors where a Higgs boson couples preferentially to vector bosons rather than to fermions.

(Submitted to Phys. Rev. D.)

---

1 Introduction

The mechanism for electroweak symmetry breaking is still a mystery. The standard model solution of a single condensing Higgs boson doublet is merely a postulate which presently happens to not be in contradiction with data. The standard model Higgs (h^0_{sm}) signatures at lepton, photon and hadron colliders have been thoroughly studied[1, 2]. Important modes of discovery have been identified, and it appears likely that a standard model Higgs boson will be seen up to about 1 TeV at the CERN LHC.

Discovery of a light h^0_{sm} is best accomplished at the CERN LEP2 e^+e^- collider, which ought ultimately to be sensitive to $m_{h^0_{sm}} \stackrel{<}{\sim} M_Z$. If 160 GeV $\stackrel{<}{\sim} m_{h^0_{sm}} \stackrel{<}{\sim}$ 800 GeV, then discovery should be possible at the CERN LHC by searching for the "gold-plated" decay $h^0_{sm} \to ZZ^{(*)} \to 4l$ which allows for a Higgs boson mass reconstruction. If $M_Z \stackrel{<}{\sim} m_{h^0_{sm}} \stackrel{<}{\sim}$ 160 GeV (the case of an intermediate mass Higgs boson), then discovery is perhaps best accomplished at the CERN LHC via a search for $h^0_{sm} \to \gamma\gamma$[3]. In the process $gg \to h^0_{sm} \to \gamma\gamma$ the total cross section peaks at about 50 fb for $m_{h^0_{sm}} \simeq 130$ GeV. The cross-section reduces to about 25 fb at $m_{h^0_{sm}} \simeq 150$ GeV. The background is continuum $q\bar{q} \to \gamma\gamma$ production, which can be overcome with excellent photon energy resolution – a feature planned for both detectors at the LHC [4].

A SM Higgs boson discovery could also be possible at the Fermilab Tevatron $p\bar{p}$ collider. Direct s-channel Higgs boson production at the Tevatron does not lead to any signals observable above background. However, by focusing on Higgs boson production in association with a vector boson ($q\bar{Q} \to Wh^0_{sm}$), a mass bump from $h^0_{sm} \to b\bar{b}$ can be reconstructed above background by also tagging on a charged lepton from the W decay. With 30 fb^{-1} of integrated luminosity it appears possible to discover the Higgs in the $l\bar{b}b$ mode at the Tevatron if its mass is below about 120 GeV [5, 6]! Discovery of a SM Higgs via the associated production mechanism is also possible at the CERN LHC [7] for $m_{h^0_{sm}} \stackrel{<}{\sim} 125$ GeV if an integrated luminosity of 30 fb^{-1} is accumulated.

Other topology searches can discover and effectively measure the mass of the light standard model Higgs boson. However, one should carefully study all possible modes of detecting the degrees of freedom arising from electroweak symmetry breaking since we do not presently know exactly how this symmetry breaking is accomplished or how it will show up experimentally. In some cases, the secondary or tertiary modes for detecting the standard model

2

Higgs boson become the most important discovery modes for the actual mechanism nature has chosen. Therefore we study another method to search for the Higgs boson. Namely, as the intermediate mass Higgs boson gets heavier, its decays into $WW^{(*)}$ get larger and can become relevant. Sometimes these decays will lead to two leptons and missing energy from $h_{sm}^0 \to WW^{(*)} \to l\nu l\nu$. If the associated W decays leptonically one is left with a trilepton signature with missing energy: $Wh_{sm}^0 \to WWW^{(*)} \to 3l + \not{E}_T$. The backgrounds to this process are small but important and will be discussed in the sections on the Tevatron and LHC search capabilities below.

The trilepton Higgs mode is unique among Higgs signatures at hadron colliders in that it occurs only by gauge interactions. Some studies have been carried out for $Wh \to l\nu\gamma\gamma$ [8, 5, 9], which is also allowed by purely gauge interactions. However, this process is usually only applicable for Higgs masses below $100\,\mathrm{GeV}$ – a mass region that can be covered effectively by LEP2 searches in the next year. The $gg \to h_{sm}^0 \to \gamma\gamma$ requires Yukawa interactions for the production, $pp \to W^{\pm}h_{sm}^0 \to l\nu b\bar{b}$ requires Yukawa interactions in the decay, and even $gg \to h_{sm}^0 \to WW^*$ studied in [10, 11, 12], which utilizes the same $h_{sm}^0 \to WW^* \to l\nu l\nu$ decay, requires Yukawa interactions in the production (unless $m_{h_{sm}^0}$ is very high and then WW fusion becomes important). Since $pp \to W^{\pm}h_{sm}^0 \to 3l$ only requires gauge interactions it could probe some Higgs bosons that the other detection modes could not if there are scalar degrees of freedom associated with electroweak symmetry breaking that have little to do with fermion mass generation. It is partly for this reason why we consider it important to study this trilepton signal.

2   Higgs decays to leptons

In the standard model the branching fractions of the Higgs boson are presented in Fig. 1. The $b\bar{b}$ mode dominates up to about $130\,\mathrm{GeV}$. Above $130\,\mathrm{GeV}$ the $WW^{(*)}$ becomes competitive and eventually dominates the decay modes of the standard model Higgs.

Each of the standard model decay modes plays an important role in standard model Higgs phenomenology. For example, the $h_{sm}^0 \to gg$ decay is directly related to the $gg \to h_{sm}^0$ production cross-section which is so important for the LHC searches. Likewise the $h_{sm}^0 \to \gamma\gamma$ mode is important as a decay mode since a peak of the $\gamma\gamma$ distribution can be resolved from
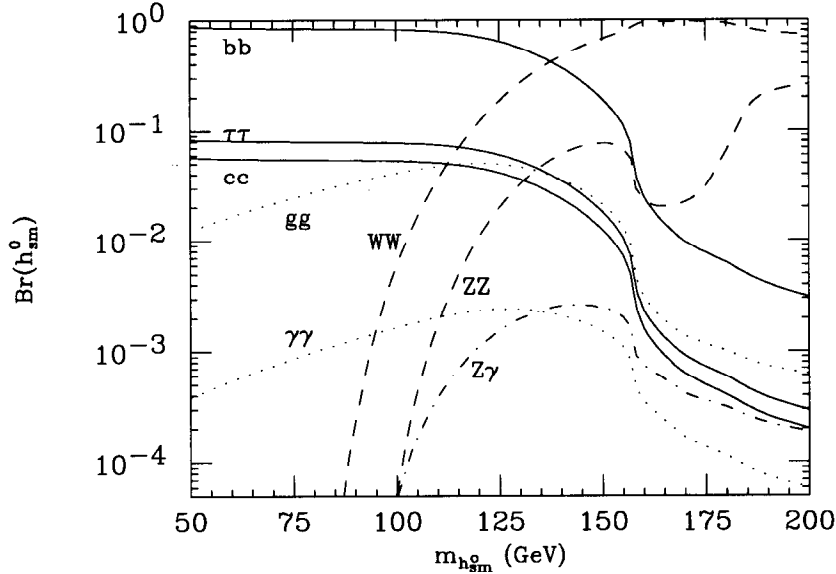
Figure 1: Decay branching fractions of the standard model Higgs boson.

background with good photon resolution. At leading order

$$\sigma(gg \to h^0_{sm} \to \gamma\gamma) \propto \Gamma(h^0_{sm} \to gg)\Gamma(h^0_{sm} \to \gamma\gamma). \tag{1}$$

The branching fraction into $ZZ^{(*)}$ becomes important for the "gold-plated" $4l$ Higgs decay mode with the invariant mass of all four leptons reconstructing the Higgs mass. At the Tevatron and also at the LHC the $W^\pm h^0_{sm} \to l\nu b\bar{b}$ mode is relevant because of the large $h^0_{sm} \to b\bar{b}$ branching fraction for a Higgs with mass below $130\,\text{GeV}$.

The gg and $\gamma\gamma$ branching fractions are loop mediated decays, and it is quite likely that they could be substantially modified if there were new physics running around the loops. In the case of supersymmetry, the present mass limits preclude the possibility of substantial alterations of standard model predictions from new particles in the loops. The most important effect in the MSSM is the extended Higgs sector which allows more complicated couplings to the standard model particles through mixing of the additional Higgses. This is especially true for large $\tan\beta$ models. Although large $\tan\beta$ models are somewhat finetuned, they nevertheless are required by some attractive $SO(10)$ grand unified models with $b - \tau - t$ Yukawa unification [13].

4

The neutral scalar Higgs mass matrix is

$$M^2 = \begin{pmatrix} m_A^2 \sin^2\beta + m_Z^2 \cos^2\beta & -\sin\beta\cos\beta(m_A^2 + m_Z^2) \\ -\sin\beta\cos\beta(m_A^2 + m_Z^2) & m_A^2 \cos^2\beta + m_Z^2 \sin^2\beta \end{pmatrix} + \begin{pmatrix} \Delta_{11} & \Delta_{12} \\ \Delta_{12} & \Delta_{22} \end{pmatrix}. \qquad (2)$$

The first term is the tree-level contribution to the mass matrix and the second term is the one loop contribution to the mass matrix. The values of the Δ's can be found in several places, including in [14]. As $\tan\beta$ gets higher the value of $m_A^2 \sin\beta\cos\beta$ gets smaller, and typically the value of Δ_{12} gets larger. Thus, it is possible to have a cancellation between the tree-level contribution and the one-loop correction such that $M_{12}^2 = 0$. In this extreme case, the two eigenvalues are pure h_u^0 and h_d^0 with masses

$$m_{h_d^0}^2 = -m_Z^2|\cos 2\beta| + \Delta_{12}\tan\beta + \Delta_{11} \qquad (3)$$

$$m_{h_u^0}^2 = m_Z^2|\cos 2\beta| + \frac{\Delta_{12}}{\tan\beta} + \Delta_{22}. \qquad (4)$$

This limit is only possible for $\tan\beta \gtrsim 30$, and so the lightest eigenvalue is well approximated by the value $m_Z^2 + \Delta_{22}$ which implies $m_{h_u^0} \gtrsim 100\,\text{GeV}$ given current squark bounds. Furthermore $\langle H_u^0 \rangle = v_u \simeq v$, and so h_d^0 acts as a spectator to electroweak symmetry breaking.

In Fig. 2 we plot the decay branching fractions for an extreme case where $h_{sm}^0 \simeq h_u^0$, versus $m_{h_u^0}$. Since the h_u^0 has no tree-level couplings to the b quarks its partial width into them is negligible. However, the partial widths to gg, $\gamma\gamma$, WW, etc. are not appreciably affected. Therefore, the branching fraction into WW^* becomes even more significant. For a Higgs mass of $100\,\text{GeV}$ the h_u^0 branching fraction into WW^* is more than eight times that of h_{sm}^0. For a Higgs mass of $120\,\text{GeV}$ this enhancement factor drops down to about four times, and for $140\,\text{GeV}$ it is a little less than a factor of two enhancement.

This suppression of the $b\bar{b}$ mode for high $\tan\beta$ models is somewhat generic even when the cancellation between the tree level and one loop corrections are not exact [15]. This is true when the tree-level and one-loop contributions are of opposite sign to each other, usually implying a particular sign for the μ parameter. The other sign of the μ parameter will generally lead to a much enhanced $b\bar{b}$ Higgs branching mode in supersymmetric models, making the WW^* decay mode less important. Discussion of supersymmetry and the light Higgs together is appropriate since it can be shown that even the most complicated Higgs sector will yield at least one light eigenvalue below about $150\,\text{GeV}$ provided the gauge couplings remain perturbative up to the GUT/Planck scale [16].
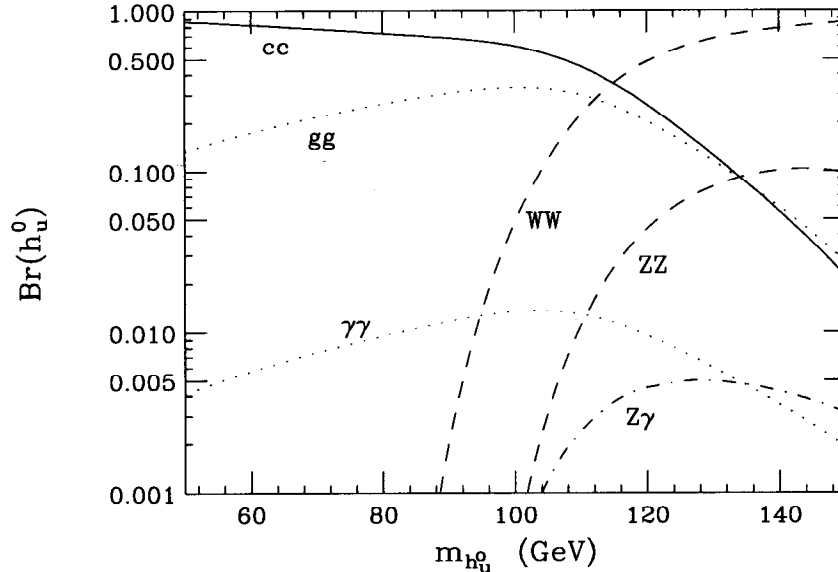
5

Figure 2: Decay branching fractions of h_u^0 Higgs boson.

Many models which have more than one degree of freedom contributing to electroweak symmetry breaking will yield non-standard model like branching fractions for the lightest Higgs particle, and can yield an enhanced WW^* branching fraction. The effect is most pronounced if fermion mass generation is largely separated from electroweak symmetry breaking – a possibility that is certainly not unreasonable [17]. In this case at least one scalar will have larger branching fractions into vector bosons than the standard model Higgs. In the extreme case of a "bosonic" Higgs, the branching fractions to $\gamma\gamma$ dominate with Higgs mass below 90 GeV and the $WW^{(*)}$ branching fractions begin to dominate for Higgs mass above that [18, 5]. Many of the results that we will show below will be using the standard model as a primary example, but it should always be kept in mind that the significance of the trilepton Higgs signal can be greatly enhanced if nature chooses a somewhat more complicated symmetry breaking pattern.

3 Trilepton Higgs signal at the Tevatron

Since single production of h_{sm}^0 via $gg \rightarrow h_{sm}^0$ does not lead to observable signals at the Fermilab Tevatron collider, the main production mode of interest for the Higgs boson is

$p\bar{p} \rightarrow W^* \rightarrow W^{\pm}h^0_{sm}$[5]. In the introduction we noted that the $l\nu b\bar{b}$ decay mode of this process has been studied in detail and it has been determined that with 30 fb^{-1} of data one could detect the Higgs boson if it had mass below 120 GeV. Above 120 GeV not only does the cross-section decrease but the branching fraction into b quarks drops as well. If there is any hope to see the standard model Higgs at the higher masses, one will need to study the more dominant decay mode $h^0_{sm} \rightarrow WW^*$ and hope that a signal above background could be found.

The subprocess total cross section for Wh^0_{sm} is given by

$$\hat{\sigma}(d\bar{u} \rightarrow W^- h^0_{sm}) = \frac{g^4 M_W^2 \lambda^{\frac{1}{2}}(\hat{s}, m^2_{h^0_{sm}}, M_W^2)|D_W(\hat{s})|^2}{192\pi\hat{s}} \left(1 + \frac{\lambda(\hat{s}, m^2_{h^0_{sm}}, M_W^2)}{12\hat{s}M_W^2}\right), \qquad (5)$$

where $\lambda(a, b, c) = a^2 + b^2 + c^2 - 2ab - 2ac - 2bc$ and $D_W(\hat{s}) = 1/(\hat{s} - M_W^2 + iM_W\Gamma_W)$. We convolute the above subprocess cross section with CTEQ4 parton distribution functions, and scale our results so that they are in accord with recently calculated NLO QCD cross section calculations[19]. In Fig. 3 the upper line shows the total next-to-leading order cross section for $p\bar{p} \rightarrow W^{\pm}h^0_{sm}$ at the Tevatron with $\sqrt{s} = 2$ TeV. Below that we have multiplied the cross-section by the branching fraction of the Higgs to decay to $WW^{(*)}$ and also multiplied by the probability that each of the three W's in the event will decay to $e\nu$ or $\mu\nu$, thus yielding a trilepton signal.

To calculate differential distributions, we calculate $q\bar{Q} \rightarrow l\bar{\nu}h^0_{sm}$ production using Monte Carlo integration. Spin correlation effects are included by using the squared matrix elements given by Baer $et\ al.$[19]. For $h^0_{sm} \rightarrow WW \rightarrow l_1\bar{\nu}_1\bar{l}_2\nu_2$ decay, we implement the spin correlated matrix element given by Barger $et\ al.$[11]. The three final state leptons are generally highly energetic and isolated. The events also have a substantial amount of missing E_T associated with them. To demonstrate this, we show in Fig. 4 the lepton p_T and missing E_T for $m_{h^0_{sm}} = 160$ GeV.

At the Tevatron the main background is expected to be from WZ production [20] where the W decays to e or μ, and the Z decays to two leptons. We include QCD corrections to our WZ background estimate[21]. To reduce backgrounds, we employ the following cuts [20]: (1) Three isolated and central ($|\eta| < 2.5$) leptons with $p_T = (20, 15, 10)$ GeV for the three leptons in descending order of p_T; (2) $\not{E}_T > 25$ GeV; (3) the invariant mass of the opposite-sign, same-flavor lepton pair not reconstruct to the Z boson mass, $|m_{l^+l^-} - m_Z| < 10$ GeV; (4) no jets in the event. The jet veto typically reduces purely electroweak sources of trileptons by
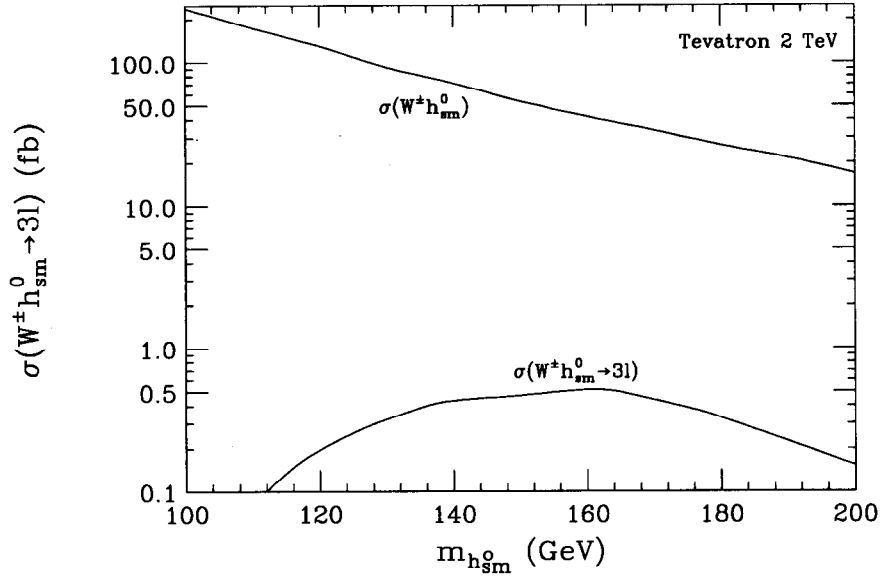
Figure 3: The upper line is the total next to leading order $W^{\pm}h^0_{sm}$ cross section at the Tevatron with 2 TeV center of mass energy. The lower line is the total three lepton cross section from $W^{\pm}h^0_{sm} \to 3l$.
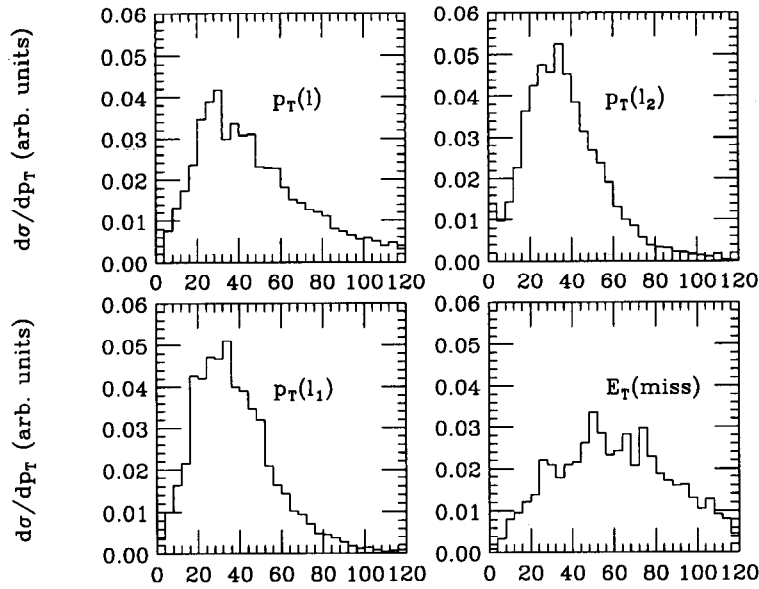

Figure 4: Lepton p_T and missing E_T distributions from $W^{\pm}h^0_{sm} \to 3l$ at the Tevatron. The Higgs mass is 160 GeV in this figure.
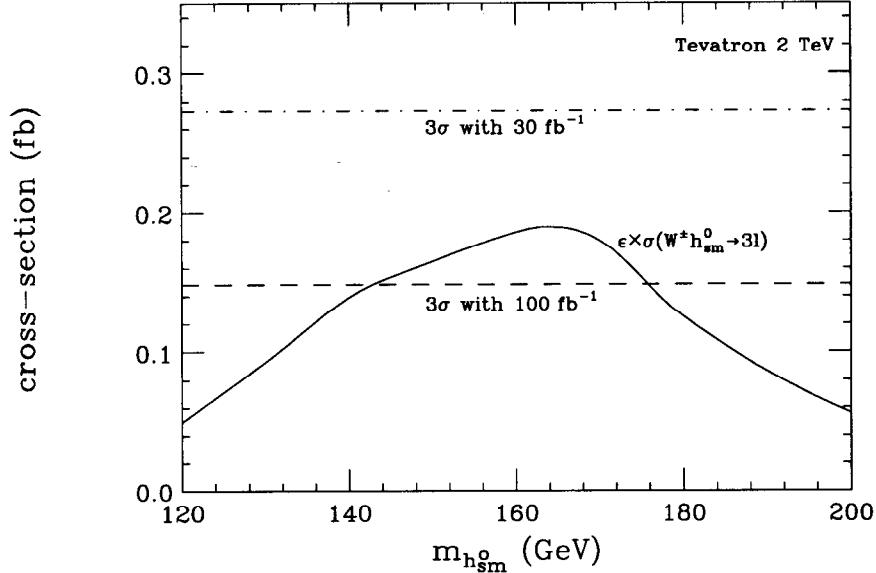
Figure 5: The solid line is the total Higgs trilepton cross-section after background reducing cuts. The dash-dotted line is the 3σ discovery contour given 30 fb^{-1} of data, and the lower line is the 3σ discovery contour given 100 fb^{-1} of data.

a factor of 2[20], while reducing $t\bar{t}$ background to levels well below that from WZ production. We incorporate a jet veto factor of 0.5 in our parton level signal generator. After all the cuts are applied the background is reduced to 0.25 fb.

In Fig. 5 we plot the trilepton signal after cuts. The reduction of the signal varies from 0.25 to 0.41 in the plotted Higgs mass range. Also in Fig. 5 we have put 3σ discovery contours for 30 fb^{-1} and 100 fb^{-1}. With 30 fb^{-1} a 3σ confidence on a discovery does not appear possible. With 100 fb^{-1} the 3σ range corresponds to about $140\,\text{GeV} \lesssim m_{h^0_{sm}} \lesssim 175\,\text{GeV}$.

The trilepton Higgs signal significance is plotted versus m_{h^0} for different Higgs models in Fig. 6. h^0_{bh} is the purely bosonic coupled Higgs boson [18, 5]; h^0_{ew} is the electroweak symmetry breaking Higgs boson of a top quark condensate model [17]; h^0_u is the "up-Higgs" of high $\tan\beta$ supersymmetry models which do not couple to down quarks or leptons; and, h^0_{sm} is the standard model Higgs boson. The non-standard Higgses have higher significance at lower Higgs mass because the branching fraction $B(h^0 \to WW^*)$ is much higher for these Higgses than the standard model Higgs. When $160\,\text{GeV} \lesssim m_{h^0} \lesssim 200\,\text{GeV}$ the branching fractions into WW^* are about the same for all Higgs models.

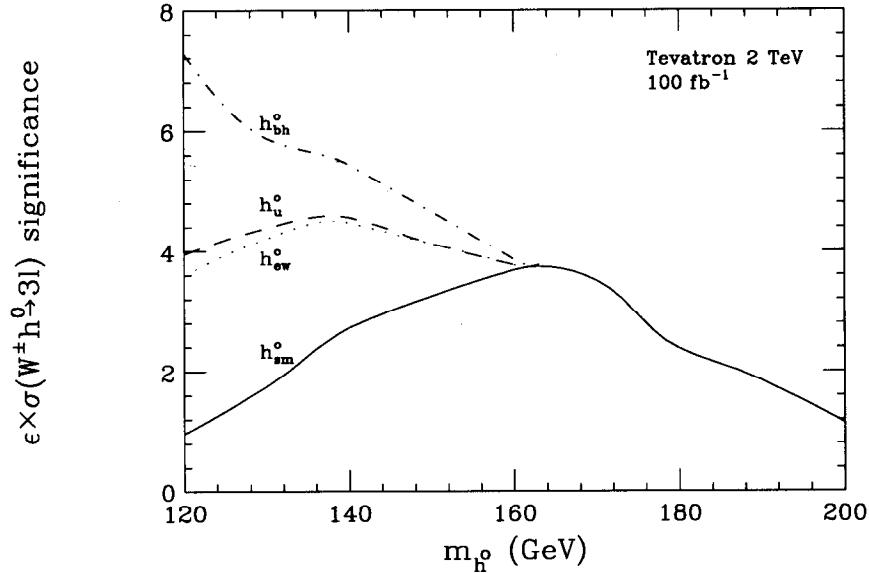Even when the signal significance is marginal, it still might be possible to extract evidence

9

Figure 6: The discovery significance for different Higgs models as a function of the Higgs mass. h^0_{bh} is the purely bosonic coupled Higgs boson; h^0_{ew} is the electroweak symmetry breaking Higgs boson of a top quark condensate model; h^0_u is the "up-Higgs" of high $\tan\beta$ supersymmetry models which do not couple to down quarks or leptons; and, h^0_{sm} is the standard model Higgs boson.

for a Higgs boson by looking carefully at the lepton kinematics on an event by event basis. For example, the main background arises from WZ when the Z decays to $\tau^+\tau^-$ and the τ's subsequently decay leptonically. In this case, the leptons from the τ decay will be softer than any of the leptons in the signal. One variable that might be useful to analyze is what we call $p_T(OS)$. It is defined to be

$$p_T(OS) = \min\{p_T(l^\pm) + p_T(l^\mp_1), p_T(l^\pm) + p_T(l^\mp_2)\}. \tag{6}$$

Among the background $WZ \to l^\pm l^\mp_1 l^\mp_2$ event sample, the unique charge lepton ($l^\pm$) must come from a lepton in the Z decay. The other two leptons with opposite charge come either from the W or Z. Generally, the lepton from the Z will be softer than the one from the W. Therefore, $p_T(OS)$ usually sums the p_T's of the two leptons which come from $Z \to \tau^+\tau^- \to l^+l^-$. In Fig. 7 we plot the distribution of $p_T(OS)$ for the WZ background (dashed line) and the signal (solid line) with $m_{h^0_{sm}} = 160\,\mathrm{GeV}$.

From Fig. 7 it is clear that the $p_T(OS)$ spectrum for the signal is much harder than that of the background. The total number of signal trilepton events expected at the Tevatron is quite
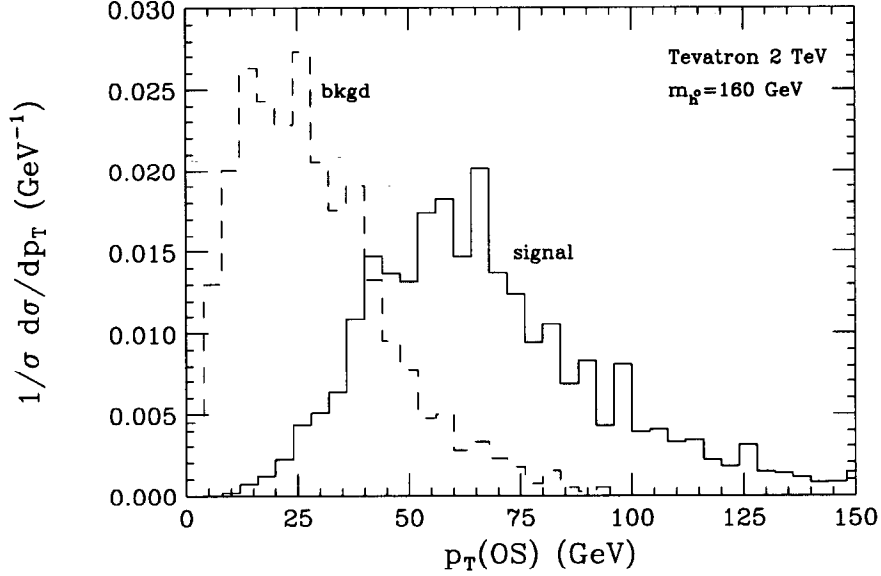
10

Figure 7: Distribution of $p_T(OS)$, which is defined to be the minimum p_T sum of opposite sign leptons in the $3l$ events. The solid line is the distribution from the $Wh^0_{sm} \to 3l$ signal, and the dashed line is the distribution from the WZ background. Events with high $p_T(OS)$ would provide strong hints for the $Wh \to 3l$ signal.

small, and as shown earlier one does not expect to get statistically compelling signal for the standard model Higgs with less than 100 fb^{-1}. However, if there are a handful of trilepton events and several of these events have $p_T(OS) \gtrsim 70\,\text{GeV}$ then this would be a powerful hint for the presence of the signal. If several events showed up with $p_T(OS) > 100\,\text{GeV}$ then the possibility that it came from WZ background fluctuations would be extremely small, and the evidence for a signal would be intriguing. To get two or more signal events with such large $p_T(OS)$ would also need to be somewhat of a lucky fluctuation. With 30 fb^{-1} the expected number of signal events after all cuts and with $p_T(OS) > 100\,\text{GeV}$ is about 0.8 events for $m_{h^0_{sm}} = 160\,\text{GeV}$. Therefore, a fluctuation of two or more signal events with $p_T(OS) > 100\,\text{GeV}$ has a reasonable probability of occurring, whereas the background has a negligible probability of producing two or more such events.
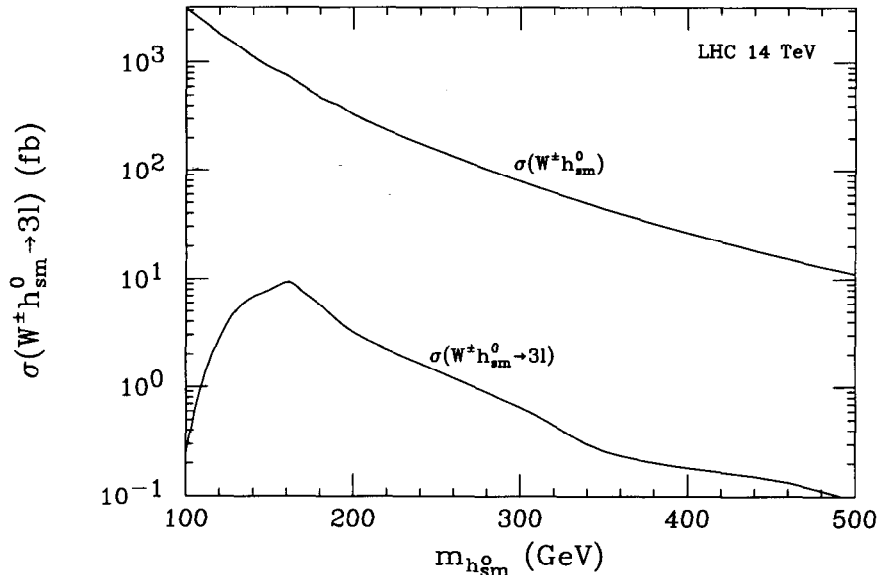
Figure 8: The upper line is the total next to leading order $W^{\pm}h^0_{sm}$ cross section at the LHC with 14 TeV center of mass energy. The lower line is the total three lepton cross section from $W^{\pm}h^0_{sm} \to 3l$.

4 Trilepton Higgs signal at the LHC

At the LHC the $gg \to h^0_{sm} \to \gamma\gamma$ mode is perhaps the most promising way to discover an intermediate mass SM Higgs boson. Indeed, even the lightest supersymmetric Higgs has excellent prospects for being discovered in this mode [22, 15]. However, other modes have been studied, and it has been shown, for example, that $W^{\pm}h^0_{sm} \to l\nu b\bar{b}$ may also be utilized to detect a Higgs if its mass is below about 120 GeV.

The trilepton Higgs signal at the LHC provides a complementary way to detect a Higgs boson in the intermediate mass region. In Fig. 8 the upper line plots the total next-to-leading order $W^{\pm}h^0_{sm}$ production cross-section for the standard model Higgs at the LHC with $\sqrt{s} = 14$ TeV. The lower line is the total three lepton cross-section after all branching fractions have been folded in. In Fig. 9 we show the lepton p_T and missing E_T distributions for $m_{h^0_{sm}} = 160$ GeV.

The lack of hadronic activity in the partonic subprocess for the signal provides a useful tool for overcoming backgrounds. The main background at the LHC is again $t\bar{t}$ and WZ production. These backgrounds can be reduced by requiring[23] (1) $p_T(l_1, l_2, l_3) >$
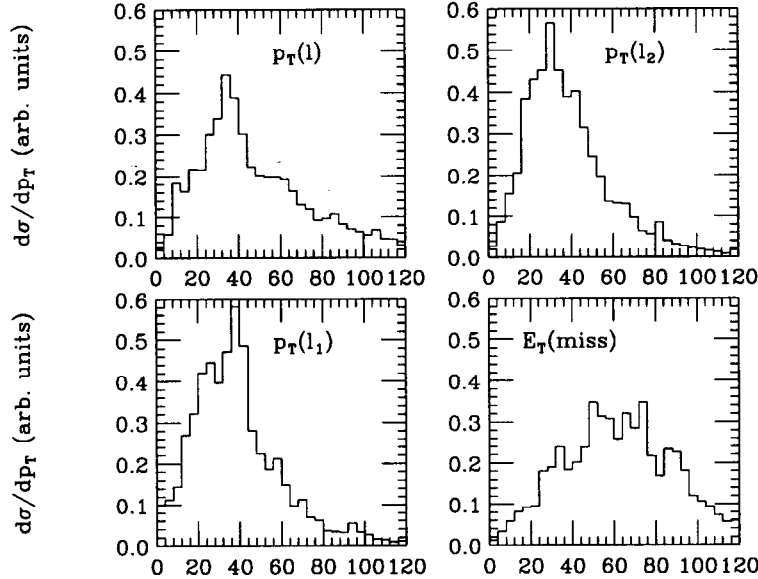
12

Figure 9: Lepton p_T and missing E_T distributions from $W^{\pm}h^0_{sm} \to 3l$ at the LHC. The Higgs mass is 160 GeV in this figure.

$(20, 20, 10)$ GeV, (2) no central ($|\eta| < 3$) jets with $p_T > 25$ GeV, (3) $|m_{l^+l^-} - m_Z| < 8$ GeV. These constitute the "soft" cuts against background of Ref. [23], leaving a total background rate of 4.3 fb. The "hard" cuts which further reduce the $t\bar{t}$ background keep events only if the two fastest leptons are the same sign and the third lepton has the same flavor as either the first or second lepton, *or* if the two fastest leptons have opposite sign and the third lepton has $p_T > 20$ GeV. With these "hard" cuts the background is reduced to 1.1 fb which mainly comes from WZ production where $Z \to \tau\bar{\tau} \to l\bar{l'} + \nu's$.

In Fig. 10 we have plotted the next-to-leading order signal cross section after employing the cuts described in the previous paragraph. The 5σ discovery contours are shown assuming 30 fb^{-1} and 100 fb^{-1}. For 30 fb^{-1} (100 fb^{-1}), it appears possible to see a Higgs trilepton signal for 140 GeV $< m_{h^0_{sm}} < 185$ GeV (125 GeV $< m_{h^0_{sm}} < 200$ GeV) at the LHC! In addition, the Higgs trilepton signal covers the difficult region 150 GeV $< m_{h^0_{sm}} < 180$ GeV where the $h^0_{sm} \to \gamma\gamma$ signal is rapidly diminishing, and $h^0_{sm} \to ZZ^*$ is proceeding at a low rate with one off-shell Z-boson.

One difficulty with the trilepton Higgs signal at the LHC is that a Higgs mass reconstruction appears difficult since there are two neutrinos in the Higgs boson decay products. However, the invariant mass of the opposite sign/same flavor dileptons from h^0_{sm} decay will
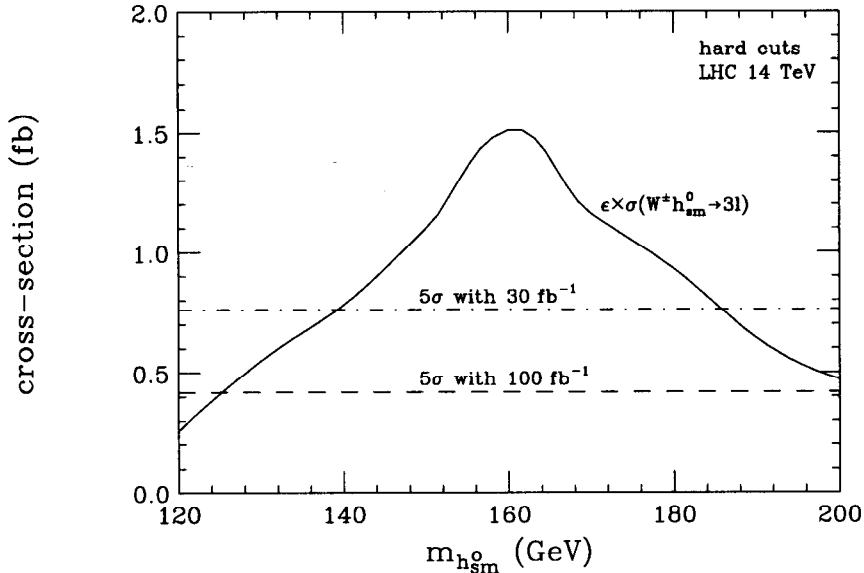
13

Figure 10: Trilepton Higgs cross-section after "hard" background reducing cuts. The 5σ discovery contours are shown assuming 30 fb^{-1} and 100 fb^{-1} of integrated luminosity.

be kinematically bounded by $m_{h^0_{sm}}$, and the distribution should scale with $m_{h^0_{sm}}$. We show the idealized distribution in Fig. 11 for several choices of Higgs boson mass. Fig. 11 always assumes the correct choice of of dilepton pair in reconstructing the invariant mass. Even for this idealized case, a mass reconstruction would be difficult given the expected number of events from a signal channel.

5   Conclusion

We have shown that a 3σ trilepton SM Higgs signal can be found at the Tevatron with 100 fb^{-1} in the range $140\,\mathrm{GeV} < m_{h^0_{sm}} < 175\,\mathrm{GeV}$. Models of electroweak symmetry breaking beyond the single Higgs postulate of the standard model may enable discovery of the Higgs with more significance at lighter masses. Furthermore, analyzing the kinematics of each detected event in the trilepton sample would add more discriminating power to the naive significance values we calculated above. Perhaps the most useful observable to analyze for this purpose is the $p_T(OS)$ variable discussed in section 3. The distribution of $p_T(OS)$ is softer for the background than for the signal, and can be used to further determine if a
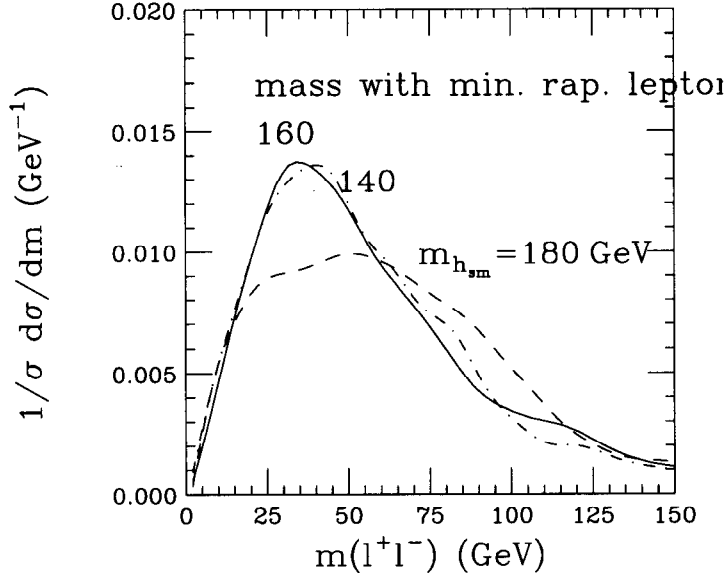
14

Figure 11: Invariant mass of opposite-sign/same flavor dilepton pairs from the higgs trilepton signal at the LHC for $m_{h^0_{sm}}$ = 140, 160 and 180 GeV.

trilepton Higgs signal is present in the data.

We also found that at the LHC with 30 fb^{-1} (100 fb^{-1}), a 5σ discovery can be made for the Higgs in the trilepton mode in the mass range 140 GeV $\lesssim m_{h^0_{sm}} \lesssim$ 180 GeV (125 GeV $\lesssim m_{h^0_{sm}} \lesssim$ 200 GeV). Reconstructing the Higgs mass will be difficult, although some guidance can be obtained by examining the invariant mass distribution of opposite-sign/same flavor dilepton pairs. Other possible techniques have been presented in Ref. [12].

Other modes associated with $W^{\pm}h^0_{sm} \to WWW^*$ might also be useful to study as confirming evidence for a signal. For example, one might be able to see an excess in like-sign dilepton samples, such as $l^{\pm}l^{\pm}jj + \not{E}_T$. Furthermore, the Zh^0_{sm} production and decay could also be useful to analyze in several channels including $Zl^+l'^- + \not{E}_T$. The statistical significance of these other modes is not as impressive as the $3l$ signal discussed above, but it might be possible to use them to bolster the claims for a signal in the $3l$ channel and to get a better handle on the Higgs mass.

Acknowledgments

15

References

[1] J. F. Gunion, H. Haber, G. Kane and S. Dawson, *The Higgs Hunter's Guide* (Addison-Wesley Publishing Company, Redwood City, CA, 1990); Electroweak Symmetry Breaking and New Physics at the TeV Scale, ed. by T. Barklow, S. Dawson, H. Haber and J. Siegrist, (World Scientific, Singapore, 1996).

[2] For a review of standard model Higgs detectability see, Z. Kunszt, S. Moretti, W.J. Stirling, Zeit. für Physik C **74**, 479 (1997); J.F. Gunion, A. Stange, S. Willenbrock, hep-ph/9602238; S. Moretti, hep-ph/9612310 .

[3] J. Gunion, G. Kane and J. Wudka, Nucl. Phys. B **299**, 231 (1988).

[4] CMS Technical Proposal, CERN/LHC/94-43 LHCC/P1 (December 1994); ATLAS Technical Proposal, CERN/LHC/94-43 LHCC/P2 (December 1994).

[5] A. Stange, W. Marciano, S. Willenbrock, Phys. Rev. D **49**, 1354 (1994), Phys. Rev. D **50**, 4491 (1994); *The TeV-2000 Group Report*, ed. by D. Amedei and R. Brock, Fermilab-Pub-96/082 (1996).

[6] S. Kim, S. Kuhlmann, W. Yao, CDF/ANAL/EXOTIC/PUBLIC/3904 (October 1996), to appear in "Proceedings of the 1996 DPF/DPB Summer Study on New Directions for High Energy Physics."

[7] P. Agrawal, D. Bowser-Chao, K. Cheung, Phys. Rev. D **51**, 6114 (1995); See also D. Froidevaux, E. Richter-Was, Zeit. für Physik C **67**, 213 (1995).

[8] R. Kleiss, Z. Kunszt and W. J. Stirling, Phys. Lett. B **253**, 269 (1991).

[9] A.G. Akeroyd, Phys. Lett. B **353**, 519 (1995).

[10] E. Glover, J. Ohnemus, S. Willenbrock, Phys. Rev. D **37**, 3193 (1988).

[11] V. Barger, G. Bhattacharya, T. Han, B.A. Kniehl, Phys. Rev. D **43**, 779 (1991).

[12] M. Dittmar, H. Dreiner, Phys. Rev. D **55**, 167 (1997).

[13] G. Anderson, S. Raby, S. Dimopoulos, L. Hall, Phys. Rev. D **47**, 3702 (1993).

[14] J. Ellis, G. Ridolfi, F. Zwirner, Phys. Lett. B **262**, 477 (1991).

[15] G.L. Kane, G. Kribs, S. Martin, J.D. Wells, Phys. Rev. D **53**, 213 (1996).

[16] G.L. Kane, C. Kolda, J.D. Wells, Phys. Rev. Lett. **70**, 2686 (1993); J.R. Espinosa, M. Quiros, Phys. Lett. B **302**, 51 (1993).

[17] J.D. Wells, Phys. Rev. D **56**, 1504 (1997).

[18] H. Haber, G. Kane, T. Stirling, Nucl. Phys. B **161**, 493 (1979).

[19] T. Han and S. Willenbrock, Phys. Lett. B **273**, 167 (1990); J. Ohnemus and W. J. Stirling, Phys. Rev. D **47**, 2722 (1993); H. Baer, B. Bailey and J. F. Owens, Phys. Rev. D **47**, 2730 (1993); S. Mrenna, C.-P. Yuan, hep-ph/9703224 (1997).

[20] H. Baer, Chih-hao Chen, C. Kao, X. Tata, Phys. Rev. D **52**, 1565 (1995).

[21] Next to leading order normalization for $W^{\pm}Z$ background at the Tevatron and LHC are extracted from J. Ohnemus, Phys. Rev. D **44**, 3477 (1991).

[22] H. Baer, M. Bisset, Chung Kao, X. Tata, Phys. Rev. D **46**, 1067 (1992); M. Spira, A. Djouadi, D. Graudenz, P.M. Zerwas, Nucl. Phys. B **453**, 17 (1995).

[23] H. Baer, C.-h. Chen, F. Paige, X. Tata, Phys. Rev. D **50**, 4508 (1994).